

Advanced wind turbine blade inspection with hyperspectral imaging and 3D convolutional neural networks for damage detection

Patrick Rizk^{a,b,c}, Frederic Rizk^d, Sasan Sattarpanah Karganroudi^{a,b}, Adrian Ilinca^{e,*}, Rafic Younes^f, Jihan Khoder^g

^a Department of Mechanical Engineering, Université du Québec à Trois-Rivières, Drummondville, QC, Canada

^b Centre national intégré du manufacturier intelligent (CNIMI), Université du Québec à Trois-Rivières, Drummondville, QC, Canada

^c Department of Mathematics, Computer Science and Engineering, Université du Québec à Rimouski, 300 allée des Ursulines, Rimouski, QC, G5L3A1, Canada

^d The Center for Advanced Computer Studies, University of Louisiana at Lafayette, Lafayette, LA, USA

^e T3E Industrial Research Group, Mechanical Engineering Department, École de Technologie Supérieure, 1100 Notre-Dame St W, Montréal, QC H3C 1K3, Canada

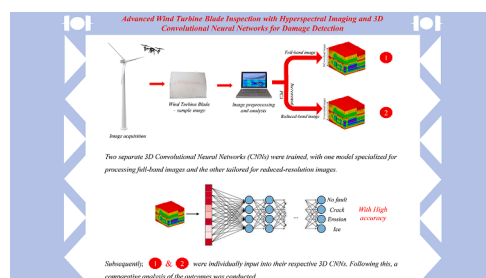
^f Faculty of Engineering, Third Branch, Lebanese University, Hadath, Beirut, Lebanon

^g LISV Laboratory, University of Versailles Saint-Quentin-en-Yvelines, 10-12 Avenue de l'Europe, 78140, Vélizy, France

HIGHLIGHTS

- Revolutionizing wind energy maintenance by integrating hyperspectral imaging and 3D CNNs for efficient wind turbine blade inspection.
- Flawless fault Detection, achieving 100 % accuracy in detecting cracks, erosion, and ice accumulation with full-band images.
- Efficiency meets accuracy; maintaining a 99.57 % accuracy while reducing dimensionality, offering practical benefits for real-world applications.
- Streamlined maintenance with a reduced training and processing times for 20-band images, promising cost savings and minimal downtime.
- A sustainable future by leveraging advanced technology for sustainable wind energy and combating climate change.

GRAPHICAL ABSTRACT



ARTICLE INFO

Keywords:

Wind turbine blade inspection
Hyperspectral imaging
3D Convolutional neural networks (CNN)
Fault detection
Wind energy sustainability

ABSTRACT

In the context of global efforts to mitigate climate change by pursuing sustainable energy sources, wind energy has emerged as a critical contributor. However, the wind energy industry faces substantial challenges in maintaining and preserving the integrity of wind turbine blades. Timely and accurate detection and classification of blade faults, encompassing issues such as cracks, erosion, and ice buildup, are imperative to uphold wind turbines' ongoing efficiency and safety. This study introduces an inventive approach that amalgamates hyperspectral imaging and 3D Convolutional Neural Networks (CNNs) to augment the precision and efficiency of wind turbine blade fault detection and classification. Hyperspectral imaging is harnessed to capture comprehensive

* Correspondence author.

E-mail address: adrian.ilinca@etsmtl.ca (A. Ilinca).

<https://doi.org/10.1016/j.egyai.2024.100366>

Available online 9 April 2024

2666-5468/© 2024 The Author(s). Published by Elsevier Ltd. This is an open access article under the CC BY-NC license (<http://creativecommons.org/licenses/by-nc/4.0/>).

spectral information from blade surfaces, facilitating exact fault identification. The process is streamlined through Incremental Principal Component Analysis (IPCA), reducing data dimensions while maintaining integrity. The 3D CNN model demonstrates remarkable performance, achieving high accuracy in detecting all fault categories in full-band hyperspectral images. The model retains high accuracy even with dimensionality reduction to 20 spectral bands. The reduced processing time of the 20-band image enhances the practicality of real-world applications, thereby reducing downtime and maintenance expenditures. This research represents a significant advancement in wind turbine blade inspection, contributing to the sustainability and dependability of wind energy systems and furthering the cause of a cleaner and more sustainable energy future as part of the broader fight against climate change.

1. Introduction

Renewable energy is a beacon of hope in pursuing sustainable energy sources to combat climate change. Nations worldwide have implemented laws and regulations to promote responsible resource utilization. Wind energy has witnessed remarkable growth during this period (Fig. 1), with a total installed wind capacity reaching 906 GW [1]. Wind turbines harness the wind’s power to generate electricity, providing an environmentally friendly alternative to fossil fuels [2]. However, despite the undeniable environmental benefits of wind energy, the industry faces a significant challenge: the maintenance and integrity of wind turbine blades [3].

Sustaining the viability and effectiveness of wind energy systems heavily relies on a pivotal component of a wind turbine: its blades. The central concern here lies in the considerable expenses and time commitments in maintenance endeavors [4,5]. Wind turbines, frequently situated in remote and rugged locales, must withstand fatigue and the unrelenting forces of nature, including wind, rain, ice, and temperature fluctuations [6]. These conditions can potentially give rise to various blade irregularities, such as cracks, erosion, and icing. These issues can lead to diminished energy output and even present safety hazards, including blade fragmentation, reduced structural integrity, vibration and imbalance, aerodynamic instability, and environmental impact [7–9]. Thus, the motivation behind this research lies within the broader context of global efforts to mitigate climate change by transitioning to renewable energy sources. As wind energy plays a pivotal role in this transition, ensuring the reliability and sustainability of wind energy systems is paramount. By addressing the maintenance challenges

associated with wind turbine blades, this study contributes to enhancing the viability and effectiveness of wind energy systems, by applying timely and accurate detection and classification of blade faults, furthering the cause of a cleaner and more sustainable energy future as part of the broader fight against climate change [10–12]. To address these maintenance challenges, extensive research and innovation efforts have been directed toward the development of methods and technologies for inspecting wind turbine blades. Particularly in cold climate regions, where ice buildup is a persistent concern, precise and efficient inspection methods are paramount [13–15].

Various methods, including ultrasound, sonic infrared (IR), thermal imaging, vibration analysis, distributed fiber optic sensors, and others, are employed for damage detection, addressing issues such as cracks, erosion, delamination, and the detection of ice, a form of surface contamination [13,16]. Few researchers, including Young et al. [17] and Rizk et al. [18,19], have explored hyperspectral imaging for blade damage detection. Young et al.’s study primarily focused on erosion detection, while Rizk et al.’s research encompassed surface damage detection and ice accretion on the blades. Additionally, other researchers have applied conventional wind turbine blades (WTB) structural health monitoring (SHM) methods with artificial intelligence (AI) techniques. This fusion of established methods with AI has enhanced accuracy in detecting faults and improved system reliability. However, there are drawbacks, such as the need for substantial data for AI training, potential false alarms, and the requirement for specialized equipment and expertise. For instance, Movsessian et al. introduced a methodology that combines vibration-based SHM with an artificial neural network (ANN). Their findings indicate that this fusion has

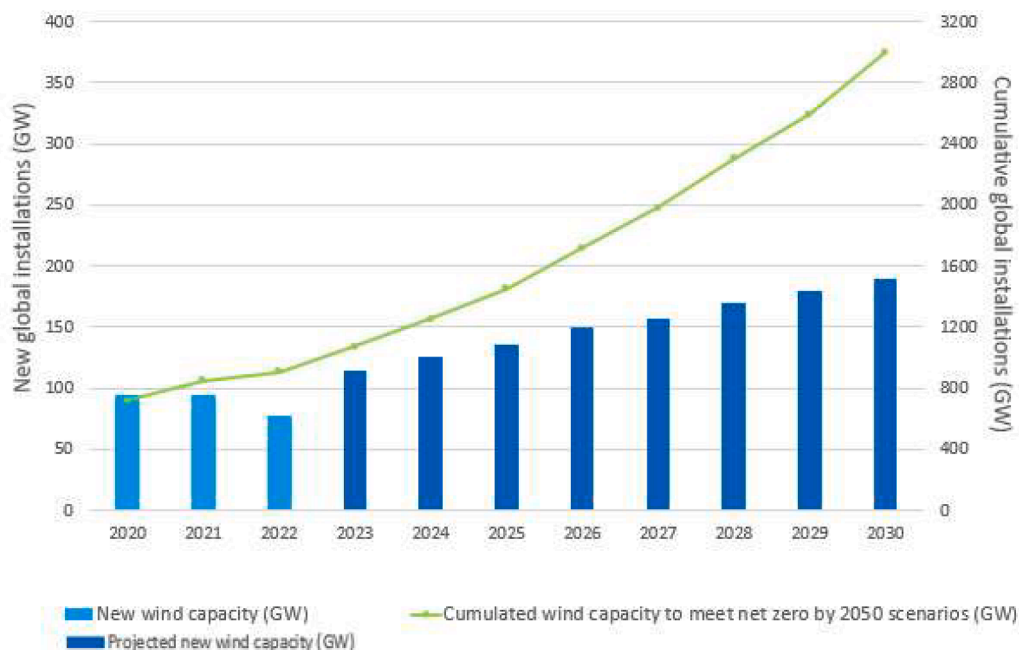


Fig. 1. Projected wind capacity 2020–2023 [1].

enhanced the detectability of damage in various scenarios they studied [20]. Additionally, AI has been applied in image processing and classification [21]. In a separate study, Reddy et al. employed convolutional neural networks (CNN) for image classification while detecting WTB damages across different categories [22]. Also, some researchers like Choung et al. [23] have proposed a system for detecting delamination faults. Zhang, Cosma, and Watkins [24] investigated deep learning algorithms for defect detection, and Wang et al. [25] introduced a multi-channel CNN for fault detection. Zhu et al. [26] developed a lightweight module architecture, and Guo et al. [27] presented a hierarchical framework for blade damage detection. Additionally, Hacıfendioğlu et al. [28] and Zare and Ayati [29] focused on ice accumulation detection and fault diagnosis using CNNs, respectively.

In recent years, a promising approach has emerged, uniting remote sensing technologies with advanced artificial intelligence techniques. This approach harnesses the capabilities of hyperspectral imaging, remote sensing data, and CNN to significantly improve the detection and classification of faults on WTB. This innovative methodology holds the potential to revolutionize blade inspection within the wind energy sector. This study introduces several groundbreaking aspects of wind turbine blade inspection. Firstly, it adopts a comprehensive approach by addressing a broad spectrum of fault types, including cracks, erosion, and ice accumulation. At the same time, other studies were limited to detecting either ice accretion or surface faults. Secondly, the integration of hyperspectral imaging and 3D CNNs enables precise fault detection by capturing detailed spectral information and considering both spatial and spectral dimensions. Moreover, the utilization of IPCA for dimensionality reduction streamlines the analysis process, enhancing its efficiency for real-world applications. Overall, this combination of techniques represents a novel and innovative approach that offers advancements in accuracy, efficiency, and practicality compared to existing methodologies. The proposed method integrates remote sensing for non-invasive monitoring of wind turbine blades with hyperspectral imaging to capture detailed spectral information about the blade's surface. Subsequently, artificial intelligence, in the form of CNN, is employed to analyze this rich data, enabling the system to automatically detect and classify various types of faults, such as cracks, erosion, and icing, with a high degree of accuracy.

The structure of this paper can be outlined as follows. In Section 1, a concise introduction to the significance of renewable energy and the challenges in wind turbine blade maintenance is provided, outlining the primary goal of the study. Section 2 presents a detailed description of the methodology, including the experimental setup and data processing. The architecture of the 3D CNN model is discussed, followed by the presentation of results and discussions in Section 3. This section showcases experimental outcomes for both classification problems, comparing the results of the 3D CNN on a full-band image and a 20-band image. Finally, in Section 4, the findings are summarized, and their implications for wind turbine blade inspection and renewable energy sustainability are discussed.

2. Hyperspectral imaging and CNN in damage detection

Hyperspectral imaging (HSI) is a cutting-edge technology that goes beyond the capabilities of the human eye. It captures detailed spectral data across a wide range of wavelengths in the electromagnetic spectrum [30]. Unlike standard imaging methods that only record three color channels (red, green, and blue), hyperspectral imaging breaks down the spectrum into many narrow, closely spaced bands. This division enables a comprehensive study of the spectral characteristics of objects and scenes [31]. For example, common wavelength ranges in hyperspectral imaging typically span from ultraviolet (UV) passing by the visible to near-infrared (NIR) or sometimes even to mid-infrared (MIR) regions, with sampled wavelength intervals as narrow as a few nanometers. This fine spectral resolution allows for precise identification and classification of various materials and objects [32]. It finds

applications in agriculture, environmental monitoring, and mineral exploration. Hyperspectral imaging offers several advantages, including early detection, non-invasiveness, and data-rich insights, making it a valuable tool in various industries for accurate monitoring and decision-making [33].

However, when coupled with CNNs, hyperspectral imaging becomes a powerful tool in damage detection and classification [21,34]. Integrating hyperspectral imaging with CNNs has revolutionized damage detection in various applications, including agriculture, environmental monitoring, and especially in the context of wind turbine blade inspections [35–37]. This innovative approach enables the early identification and classification of structural issues such as cracks, erosion, delamination, and even ice accumulation on wind turbine blades [7,38]. In this study, the potential of hyperspectral imaging is harnessed to train the CNN model, enabling it to analyze detailed spectral signatures and automatically identify and categorize damage types on a sample of WTB. This improves fault detection accuracy and streamlines the inspection process, reducing downtime and cutting maintenance costs in critical industries [39].

Nevertheless, it's worth noting that hyperspectral imaging generates substantial data due to its contiguous band, leading to challenges in data redundancy and memory requirements [32,40]. The high dimensionality of hyperspectral data not only presents significant computational burdens but also exacerbates the curse of dimensionality, particularly in the context of training complex models like 3D CNNs. While HSI offers benefits in capturing spatial and spectral information simultaneously, 3D CNNs introduce impediments such as increased computational complexity and longer training times. Thus, our study integrates dimensionality reduction techniques with 3D CNNs to address these challenges, aiming to alleviate memory constraints and enhance model efficiency.

2.1. Data description and methodology

In this study, the analysis focused on a glass fiber-reinforced plastic (GFRP) WTB sample, as depicted in Fig. 2. The sample measures 53.0 cm in length, 34.5 cm in width, and 4.0 cm in thickness, adhering to pre-existing industry standards. A spectroradiometer covering a spectral range from 340 to 1700 nm was utilized to capture the essential spectral information for the research. The investigation identified common faults in WTBs, including cracks, erosion, and ice accumulation. Table 1 provides a summary of these common faults. Each fault type is described in terms of its characteristics and potential impact on the performance and structural integrity of the blade.

After scanning the WTB sample, rigorous preprocessing techniques were applied to the hyperspectral imaging (HSI) data. This preprocessing was crucial to eliminate noise and mitigate the influence of external light sources on the image. The resultant image is represented in a

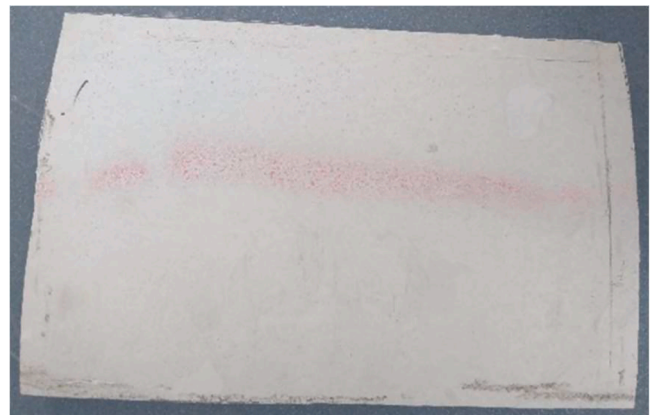


Fig. 2. Studied WTB sample.

Table 1
Summary of the studied defects.

DEFECT TYPE	CHARACTERISTICS	DEFECT SIZE	POTENTIAL IMPACT
CRACK	Visible fractures or fissures on the surface	0.3 mm	Compromised structural integrity Potential for catastrophic failure
EROSION	Surface degradation, often in the form of wear	Light erosion	Reduction in aerodynamic efficiency Increased risk of blade imbalance and vibration Decreased overall performance and lifespan
ICE ACCRETION	Accumulation of ice or frost on the surface of WTB	0.5 mm	Increased weight and imbalance Disturbance of aerodynamic properties Risk of ice shedding and damage to surrounding structures

datacube of 44 by 29 in spatial dimensions spread across a spectral dimension of 542 bands (see Fig. 3a). Fig. 3a illustrates the distribution and change in pixel intensity at each waveband. In contrast, Fig. 3b shows the scatter distribution of these intensities across the spatial dimension of the WTB at a wavelength of 1200 nm.

The 3D scatter plot of intensity distribution at 1200 nm, as depicted in Fig. 3b, serves as a valuable visualization tool that offers insights into the spectral characteristics of the inspected WTB at this specific wavelength. In this plot, each point corresponds to a pixel on the WTB's surface, and its position represents both its spatial coordinates and the intensity of reflected light at the 1200 nm wavelength.

This scatter plot effectively highlights the variations in intensity across the surface of the WTB at 1200 nm. These variations can indicate areas warranting attention, potentially signaling defects or irregularities. When examining the plot, clusters of points may suggest regions of uniformity, while outliers could signify anomalies.

2.1.1. Preprocessing pipeline

As mentioned earlier, the dataset used in this study comprises hyperspectral images obtained from WTB surfaces within a controlled laboratory setting. It encompasses instances representing three distinct classes of blade surface defects: 30 instances of cracks, 35 instances of erosion, and 198 instances of icing spots, as described in Table 1. The hyperspectral images underwent a comprehensive preprocessing pipeline. Initially, spatial patches were extracted from the preprocessed hyperspectral images to generate input samples for model training and testing. The dataset was then divided into training and testing sets using an 80/20 split ratio to ensure a balanced representation of each defect class in both sets. Subsequently, upon achieving satisfactory detection and classification performance, Incremental Principal Component Analysis (IPCA) was utilized to reduce the dimensionality of the hyperspectral data while retaining relevant information. The reduced model was then re-evaluated and compared with the full-band model. Python served as the primary programming language for model

development and evaluation, leveraging libraries such as NumPy, scikit-learn, Keras with TensorFlow backend, and matplotlib/seaborn for data manipulation, preprocessing, model implementation, evaluation, and visualization, respectively. This methodology ensures reproducibility and compatibility with established tools and practices in the field.

2.2. Dimensionality reduction

However, the rich information within the 3D datacube may impose a heavy processing load and impede data analysis. Therefore, dimensionality reduction becomes necessary. A central component of the approach involved reducing dimensionality, which played a crucial role in streamlining data processing and analysis [41]. Incremental Principal Component Analysis (IPCA) was employed for this purpose, leveraging its capability to handle massive datasets that cannot be easily accommodated in memory simultaneously. Building upon traditional Principal Component Analysis (PCA) principles, IPCA processes data in smaller batches or mini batches, allowing for an incremental approach to computing the principal components. In IPCA, data is divided into manageable masses, and the algorithm incrementally updates its calculations as it iterates through these batches [42]. This ensures the efficient extraction of the essential patterns and a reduction of the dimensionality of the data without requiring extensive memory resources. IPCA is a technique that systematically reduces data dimensionality while preserving the most relevant information [43]. Importantly, a manual-automated hybrid approach was integrated, where spectral down sampling was initially explored manually to reduce the number of bands. Subsequently, IPCA was applied to further reduce dimensionality, resulting in the selection of the first 20 representative bands based on iterative experimentation. This approach allowed for effectively balancing computational efficiency with detection and classification performance [44–46]. By implementing IPCA in conjunction with spectral downsampling, the hyperspectral data's dimensionality was successfully reduced, making it more manageable for subsequent

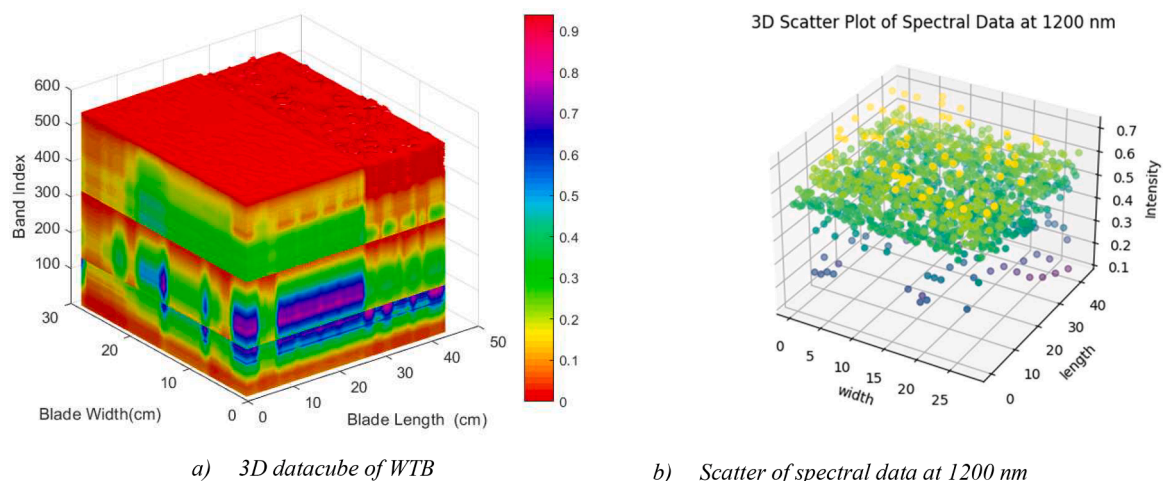


Fig. 3. 3D representation of WTB specimen.

analysis [47]. This hybrid approach not only optimized computational resources but also enhanced the accuracy of wind turbine blade fault classification.

2.3. 3D CNN architecture

After inspecting the WTB sample, artificial intelligence (AI), specifically CNNs, was employed to enhance the accuracy of the analysis. This includes using 3D CNNs, a specialized type of CNN designed for tasks involving both spatial and temporal data [48].

CNNs have gained recognition in image analysis for their ability to automatically extract intricate features from visual data [49]. The research utilizes CNNs to process the hyperspectral images captured during WTB inspections. This technology empowers the detection and categorization of various types of blade damage, such as cracks, erosion, and ice accumulation, with exceptional precision.

What sets the approach apart is the utilization of 3D CNNs. While traditional 2D CNNs excel in recognizing patterns within individual images, 3D CNNs take it a step further by considering the temporal dimension as well [50,51]. In this case, the temporal dimension corresponds to the sequence of hyperspectral images recorded during the inspection.

3D CNNs in the study work by applying 3D convolutional filters that analyze spatial features within each hyperspectral image and consider how these features evolve across the sequence of images. This capability proves particularly valuable when inspecting WTBs, as it enables the capture of static spectral characteristics and any dynamic changes in the blade's condition over time. For instance, it assists in detecting subtle variations in blade health and identifying patterns associated with damage progression.

The 3D CNN architecture employed in this study for HSI analysis consists of multiple layers designed to effectively capture spatial and spectral features from the input data (Fig. 4). The model pre-requisites involve reshaping the input data into a suitable format for training and validation purposes. Specifically, the training data and validation data are reshaped into 5D arrays with dimensions (batch_size, spatial_height, spatial_width, spectral_bands, channels), where the spatial dimensions are set to 11×11 , and the spectral bands are set to 50. Additionally, the categorical labels corresponding to the training data and validation data are one-hot encoded.

The model structure begins with an input layer that takes the 5D input data as input. Subsequently, a series of 3D convolutional layers are employed to extract spatial and spectral features from the input data. These convolutional layers utilize different filter sizes to capture features at multiple scales. Specifically, the first convolutional layer consists of 8 filters with a kernel size of $3 \times 3 \times 7$, the second convolutional layer consists of 16 filters with a kernel size of $3 \times 3 \times 5$, the third convolutional layer consists of 32 filters with a kernel size of $3 \times 3 \times 3$, and the fourth convolutional layer consists of 64 filters with a kernel size of $3 \times 3 \times 3$. Each convolutional layer applies the rectified linear unit

(ReLU) activation function.

Following the convolutional layers, a flatten layer is utilized to transform the output of the convolutional layers into a one-dimensional vector. This vector is then fed into fully connected layers, consisting of two dense layers with 256 and 128 units, respectively. Each dense layer is followed by a dropout layer with a dropout rate of 0.4 to prevent overfitting.

The Adam optimizer is employed with a learning rate of 0.001 to control the rate at which the model weights are updated during training. Finally, the output layer consists of three units with a Softmax activation function, representing the probabilities of the input belonging to each of the three fault classes: cracks, erosion, and ice accretion. This architectural design offers a robust method for extracting features from HSI data, holding potential for various applications in remote sensing and image analysis tasks. The model is summarized in Table 2.

2.4. D. comparison methods and performance evaluation

The comparative analysis presented in this paper encompasses a diverse range of classification methodologies, incorporating both modern deep-learning techniques and traditional machine-learning algorithms. Alongside the sophisticated deep learning method, the study evaluates the performance of the Support Vector Machine (SVM) as a representative of classical machine learning approaches known for their robustness and interpretability. Additionally, the analysis extends to include the Gradient Boosting method, which excels in ensemble learning by iteratively improving the predictive accuracy.

2.5. SVM

The SVM classifier implemented in this study is a widely-used machine learning algorithm renowned for its effectiveness in solving classification problems. SVM operates by identifying an optimal hyperplane that maximally separates different classes in the input data space,

Table 2
Model summary.

Layer	Output Shape	Number of Parameters
Input Layer	11, 11, 542, 1	0
Conv3d_1 (Conv3D)	9, 9, 536, 8	512
Conv3d_2 (Conv3D)	7, 7, 532, 16	5776
Conv3d_3 (Conv3D)	5, 5, 530, 32	13,856
Conv3d_4 (Conv3D)	3, 3, 528, 64	55,360
Flatten_1 (Flatten)	304,128	0
Dense_1 (Dense)	256	77,857,024
Dropout_1 (Dropout)	256	0
Dense_4 (Dense)	128	32,896
Dropout_3 (Dropout)	128	0
Dense_5 (Dense)	Number of classes	387

In total, 77,965,811 trainable parameters are essential.

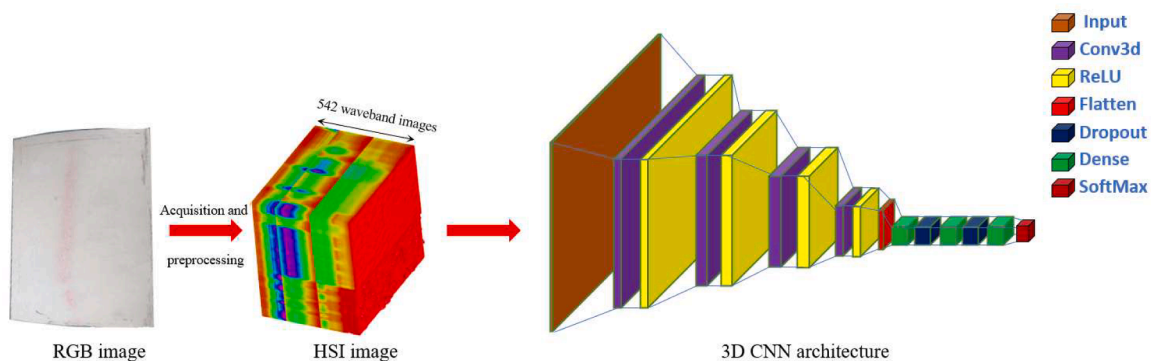


Fig. 4. HSI-CNN model architecture.

thereby facilitating accurate classification [52]. In this work, the SVM classifier is configured with the radial basis function (RBF) kernel, which enables it to effectively capture complex nonlinear relationships present in the data. By leveraging the RBF kernel and employing appropriate hyperparameters, the SVM classifier is trained on the provided dataset, enabling it to discern signatures and make detections.

2.6. Gradient boosting classifier

The gradient boosting classifier employed in this study is a group of learning technique that iteratively improves the predictive accuracy by combining multiple weak learners, typically decision trees, into a strong predictive model. It allows for fine-tuning of hyperparameters such as the number of estimators and the learning rate. During training, the classifier learns from the mistakes of its predecessors by focusing on the samples that were misclassified, thereby progressively refining its predictions [53]. This approach results in an adaptive model capable of capturing complex relationships within the data.

2.7. Performance evaluation

To evaluate the efficacy of the detection model presented in this study, two metrics, precision rate (PR) and recall rate (RR), are utilized, each quantified by specific equations.

$$PR = \frac{TP}{TP + FP} \times 100 \%, \tag{1}$$

Precision rate (PR), expressed in Eq. (1), measures the proportion of correctly identified positive instances relative to all instances identified as positive, denoted as true positives (TP) over the sum of true positives (TP) and false positives (FP).

$$RR = \frac{TP}{TP + FN} \times 100 \%, \tag{2}$$

Similarly, recall rate (RR), defined in Eq. (2), evaluates the ability of the model to identify all relevant instances, calculated as the ratio of true positives (TP) to the sum of true positives (TP) and false negatives (FN). These metrics provide insight into the model’s ability to correctly identify positive instances while minimizing false classifications.

$$F_{\beta} = (1 + \beta^2) \frac{PR * RR}{\beta^2 * PR + RR} \times 100 \%, \tag{3}$$

Furthermore, to offer a comprehensive assessment of the detection model’s performance, an F-score is computed, combining precision rate and recall rate into a unified metric. The F-score, expressed in Eq. (3), incorporates a positive real parameter, “ β ”, enabling the adjustment of emphasis between precision and recall rates. When “ β ” equals 1, the F-score corresponds to the harmonic mean of precision and recall, commonly referred to as the F1 score, providing a balanced evaluation of the model’s overall effectiveness.

3. Results and discussion

In this section, we present the results of the fault detection and classification procedure, comparing them with the outcomes after band reduction using IPCA. This research was conducted on Google Colab, where the study leveraged a Tesla T4 GPU specifically designed for machine learning and deep learning tasks. This powerful GPU boasts 2560 CUDA cores, 16 GB of GDDR6 VRAM, and Tensor Cores that enhance the efficiency of deep learning processes [54]. To ensure the accuracy and efficiency of this experiment, a division of the dataset into a 20 % test and an 80 % training split, maintaining consistency throughout the study.

As mentioned earlier, three distinct faults are investigated. They were categorized into specific classes as illustrated in the ground truth image presented in Fig. 5. Erosions were denoted by a dark grey label,

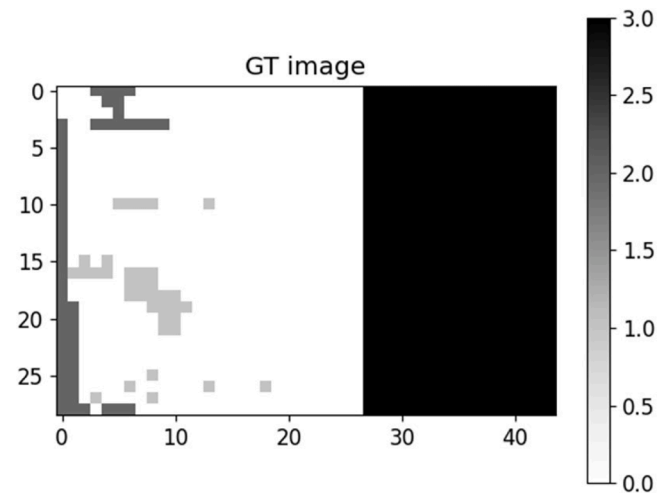


Fig. 5. Multi-class image of the WTG.

cracks by a light grey label, and ice was indicated by a black label.

To assess the capabilities of the CNN, a full-band image comprising 542 waveband images was initially employed. Then, the results were compared with two benchmark classifiers that are presented in Table 3, illustrating the performance metrics of each classifier on the dataset. These metrics include accuracy, precision, recall, and F1-score, providing a detailed analysis of the classifiers’ effectiveness in classification tasks. Subsequently, IPCA was applied to the hyperspectral image to reduce the dataset’s size used during training, thus reducing processing time. Following the application of IPCA, 20 waveband images were retained. The network’s performance was then comprehensively evaluated and compared to the results obtained using the full-band (FB) image.

When evaluating the performance of the proposed classification model, insights are drawn from a confusion matrix, presented in Fig. 6. This tool provides a detailed breakdown of how well our model identifies and classifies these critical faults through the full-band image.

In the case of crack detection, the results from the confusion matrix are undeniably remarkable. The model exhibits a perfect score, indicating a 100 % agreement between the true presence of cracks and the model’s predictions. In other words, every instance of a crack is correctly identified, underscoring the model’s proficiency in preserving the structural integrity of the turbine blades.

Similar excellence is observed in the instance of ice detection. The confusion matrix reveals a flawless 100 % true positive rate, signaling that the model accurately categorizes all cases of ice accumulation. This high level of performance is instrumental in averting ice-related issues and ensuring uninterrupted energy production.

For erosion detection, the model also achieves a remarkable 100 % true positive rate, signifying that the model accurately identifies all

Table 3
Comparison results with benchmark classifiers.

Model	Metric	Crack	Erosion	Ice	Average
SVM	Precision (%)	85	83	90	86
	Recall (%)	80	81	85	82
	F1 score (%)	83	82	88	84
	Accuracy (%)	–	–	–	84
Gradient Booster	Precision (%)	87	99	99	95
	Recall (%)	93	91	98	94
	F1 score (%)	90	95	99	95
	Accuracy (%)	–	–	–	95
Our model	Precision (%)	100	100	100	100
	Recall (%)	100	100	100	100
	F1 score (%)	100	100	100	100
	Accuracy (%)	–	–	–	100

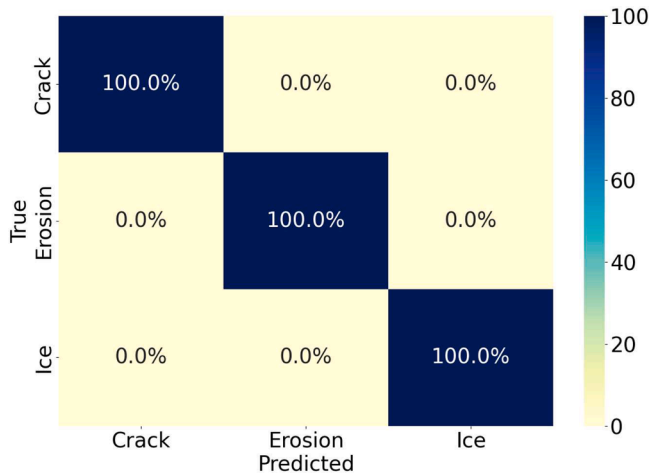


Fig. 6. Full-band image confusion matrix.

instances of erosion. This level of accuracy is highly promising, as it indicates that the model is adept at recognizing erosion-related faults on the wind turbine blades.

The convergence accuracy and loss for a full-band image of our 3D CNN model over 50 epochs are illustrated in Fig. 7 and Fig. 8, respectively. A careful examination of these figures reveals a clear trend: the proposed model converges to its optimal performance state at approximately the 25th epoch.

After employing IPCA to select the most informative 20 spectral bands from the original 542, thus significantly reducing dimensionality, the comprehensive evaluation presented in Fig. 9 via the confusion matrix encapsulates the culmination of the work.

This matrix examined three critical fault categories – crack, erosion, and ice. When considering the detection of cracks, our model exhibited a 92.9 % true positive rate, attesting to its capability to discern these structural irregularities with impressive precision. While this achievement is noteworthy, a 7.1 % misclassification rate, where true cracks were inadvertently identified as erosion, reveals an area for potential enhancement.

The evaluation of erosion detection presented a remarkable revelation. With the 20-band image, our model also achieved a perfect 100 %

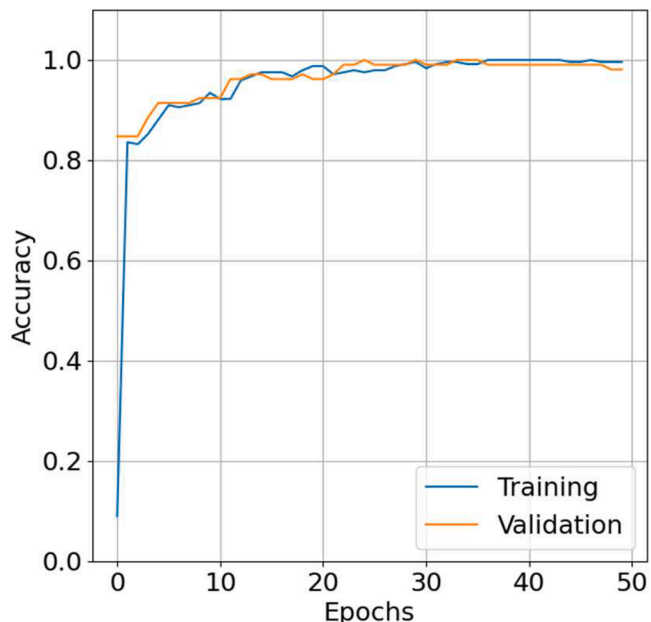


Fig. 7. FB training and validation accuracies versus epochs.

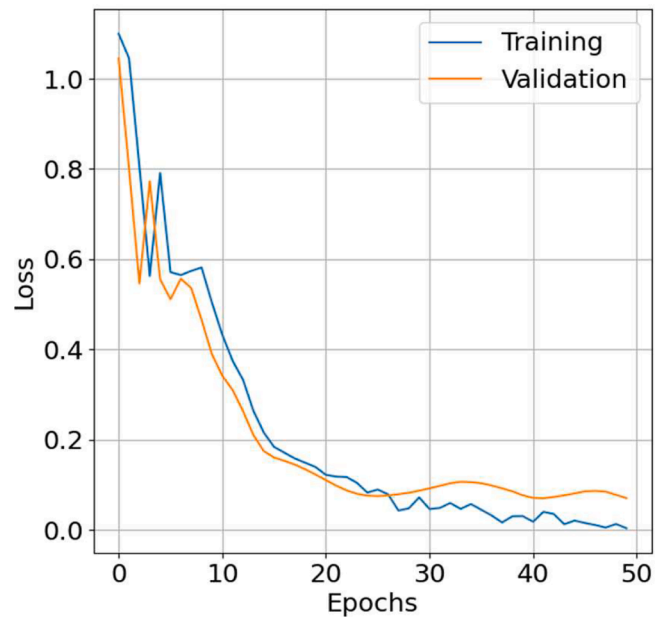


Fig. 8. FB training and validation losses versus epochs.

true positive rate, signifying its unwavering proficiency in identifying this crucial fault type. In the case of ice, the model’s performance was equally impeccable, recording a flawless 100 % true positive rate, underscoring its dependability in detecting ice-related issues.

The true achievement, however, emerged with the implementation of dimensionality reduction via IPCA. In this transformation, the spectral bands were carefully reduced from 542 to 20 bands. The impact on detection and classification was nothing short of remarkable, as the confusion matrix presents. The model exhibited a flawless 100 % true positive rate for all three fault categories - crack, erosion, and ice – in an FB image. At the same time, it maintains this rate for a 20-band image in the case of erosion and ice and an excellent rate in the case of crack.

The convergence accuracy and loss of our 3D CNN model over 50 epochs, using a 20-band image, are depicted in Fig. 10 and Fig. 11, respectively. A careful analysis of these graphical representations unveils a discernible pattern: the proposed model attains its optimal performance state at approximately the 21st epoch, particularly concerning accuracy.

Table 4 provides a comprehensive summary of the key metrics used to evaluate the performance of the 3D CNN. These metrics are crucial in assessing the model’s effectiveness and efficiency.

Test Accuracy reflects the model’s ability to correctly classify faults, with the FB image achieving a remarkable 100 % accuracy and the 20-band image maintaining an impressively high accuracy of 99.57 %. This metric showcases the model’s precision in identifying and categorizing blade damage.

Precision measures the proportion of true positive predictions among all positive predictions. Both FB and 20-band images exhibit exceptional precision, with values of 1.00 and 0.99, respectively. This indicates that the model makes accurate predictions while minimizing false positives.

Recall signifies the proportion of true positive predictions out of all actual positive instances. The FB image achieves a perfect recall of 1.00, while the 20-band image maintains a high recall rate of 0.98. This underscores the model’s ability to effectively detect all instances of blade damage.

F1-score is the harmonic mean of precision and recall, providing a balanced assessment of the model’s performance. Both FB and 20-band images yield impressive F1-scores of 1.00 and 0.98, respectively, reflecting the model’s strong overall performance.

Considering the practical implementation aspect, the reduced

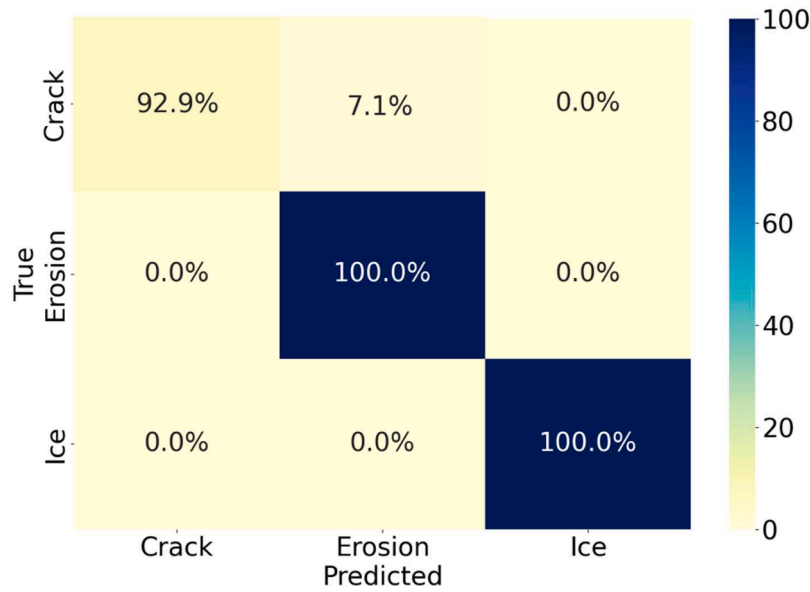


Fig. 9. 20-band image confusion matrix.

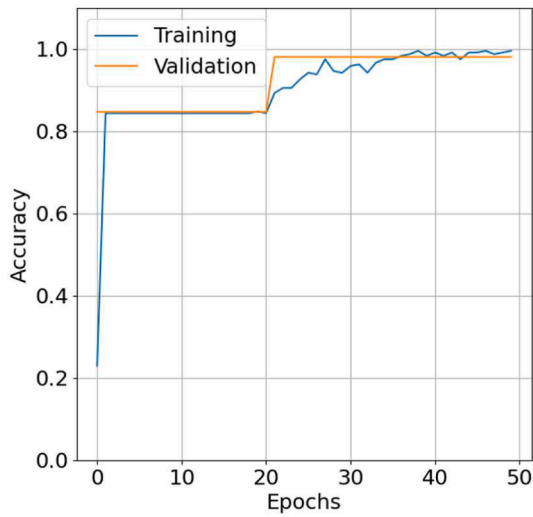


Fig. 10. 20-band image training and validation accuracies versus epochs.

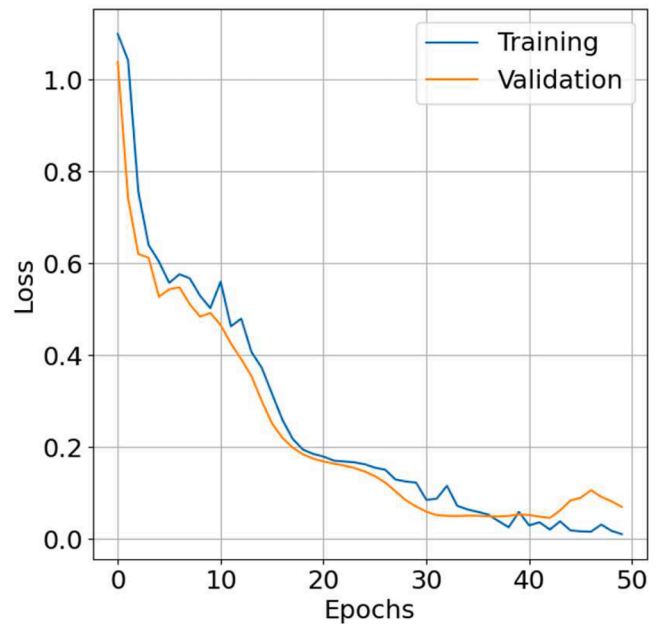


Fig. 11. 20-band image training and validation losses versus epochs.

Training Time and Processing Time associated with the 20-band image make it a viable choice for real-world applications. This efficiency could significantly benefit industries reliant on timely fault detection and inspection processes.

In summary, these metrics affirm the effectiveness of the 3D CNN model in fault detection and classification. The slight reduction in accuracy with the 20-band image is offset by its practical advantages in terms of efficiency. These results mark a significant stride in applying deep learning and hyperspectral imaging for wind turbine blade inspection, offering potential benefits for industries reliant on accurate and timely fault detection.

4. Conclusion

In conclusion, the integration of hyperspectral imaging and 3D CNNs in WTB inspection represents a significant advancement aimed at improving accuracy, efficiency, and practicality in fault detection and classification. This innovative approach holds promise for enhancing the sustainability and reliability of wind energy systems. By leveraging detailed spectral data provided by hyperspectral imaging, nuanced

Table 4

Comparison of FB vs 20-band image classification: Test Accuracy, Precision, Recall, F1-score, Training Time, and Processing Time.

Metrics	FB image	20-band image
Test Accuracy (%)	100.00	99.57
Precision	1.00	0.99
Recall	1.00	0.98
F1-score	1.00	0.98
Training Time (s)	75.4199	27.8407
Processing Time (s)	0.5146	0.4796

information about wind turbine blade surfaces can be captured, enabling early detection and precise classification of faults such as cracks, erosion, and ice accumulation, critical concerns in wind energy maintenance that can lead to costly downtime if left undetected. To

address the challenges posed by the substantial data generated by hyperspectral imaging, IPCA was implemented for dimensionality reduction, streamlining data analysis processes and reducing training time by 63.1 % and processing times by 3.5 %, thereby making the methodology more practical for real-world applications. Findings demonstrate exceptional capabilities of the CNN model in detecting and categorizing blade faults, achieving perfect performance with 100 % accuracy in detecting cracks, erosion, and ice accumulation even when reducing dimensionality to 20 bands, maintaining an impressive accuracy of 99.57 %. The reduced training and processing times associated with the 20-band image render it an attractive choice for industries reliant on timely fault detection and inspection processes, leading to cost savings and minimal downtime, thereby enhancing the viability of wind energy as a sustainable power source. Regarding practical application, integrating drone-based imaging into the pipeline for autonomous predictive maintenance presents a feasible solution. By deploying drones equipped with hyperspectral imaging sensors for regular aerial inspections of wind turbine blades, early signs of faults can be detected and analyzed using advanced machine learning algorithms. This data can then be integrated into a predictive maintenance system, enhancing maintenance efficiency and turbine performance. Furthermore, the proposed approach enhances practicality by addressing the problem of uniformity in wind turbine blade material composition and shape. The model's adaptability to variations in spectral signatures ensures its applicability without the need for reimplementation, offering a robust solution for fault detection across different blade materials. Looking ahead, future work may involve deploying computer vision techniques and studying detection in motion rather than in a controlled laboratory environment, offering opportunities for further refinement and applicability of the methodology in real-world scenarios, considering external factors like lighting conditions, rotor movement, and real blade structure. With advancements in remote sensing technologies and artificial intelligence, significant strides can be made in ensuring the integrity and longevity of wind energy systems, contributing to combating climate change and securing a sustainable energy future.

Funding

The authors declare that the research conducted in this project was supported by Natural Sciences and Engineering Research Council of Canada (NSERC) grants with reference numbers RGPIN-2023-05578, DGEGR-2023-00336, and RGPIN-2019-04220.

CRediT authorship contribution statement

Patrick Rizk: Conceptualization, Data curation, Formal analysis, Methodology, Software, Writing – original draft. **Frederic Rizk:** Formal analysis, Investigation, Software, Validation. **Sasan Sattarpanah Karganroudi:** Funding acquisition, Investigation, Project administration, Supervision. **Adrian Ilinca:** Conceptualization, Funding acquisition, Project administration, Supervision, Writing – review & editing. **Rafic Younes:** Conceptualization, Data curation, Investigation, Methodology. **Jihan Khoder:** Investigation, Methodology, Software.

Declaration of competing interest

The authors declare that they have no known competing financial interests or personal relationships that could have appeared to influence the work reported in this paper.

Data availability

Data will be made available on request.

References

- [1] *Global Wind Report 2023*. 2023, GLOBAL WIND ENERGY COUNCIL (GWEC).
- [2] Issa M, et al. Maritime Autonomous Surface Ships: problems and Challenges Facing the Regulatory Process. *Sustainability* 2022;14(23):15630.
- [3] Sheng S, O'Connor R. Chapter 14 - Reliability of wind turbines. In: Letcher TM, editor. *Wind energy engineering* (Second edition). Academic Press; 2023. p. 195–211. Editor.
- [4] Hsu J-Y, et al. Wind turbine fault diagnosis and predictive maintenance through statistical process control and machine learning, 8. *Ieee Access*; 2020. p. 23427–39.
- [5] Mishnaevsky Jr L, Thomsen K. Costs of repair of wind turbine blades: influence of technology aspects. *Wind Energy* 2020;23(12):2247–55.
- [6] García Márquez FP, Peco Chacón AM. A review of non-destructive testing on wind turbine blades. *Renew Energy* 2020;161:998–1010.
- [7] Rizk P, et al. Hyperspectral imaging applied for the detection of wind turbine blade damage and icing. *Remote Sensing Applications: Society and Environment* 2020; 18:100291.
- [8] Yang X, et al. Image recognition of wind turbine blade damage based on a deep learning model with transfer learning and an ensemble learning classifier. *Renew Energy* 2021;163:386–97.
- [9] Martini F, et al. Turbulence modeling of iced wind turbine airfoils. *Energies* 2022; 15(22):8325.
- [10] Wang W, et al. Review of the typical damage and damage-detection methods of large wind turbine blades. *Energies* 2022;15(15):5672.
- [11] Du Y, et al. Damage detection techniques for wind turbine blades: a review. *Mech Syst Signal Process* 2020;141:106445.
- [12] Contreras Montoya LT, et al. 4 - Renewable energy systems. In: Kabalci E, editor. *Hybrid renewable energy systems and microgrids*. Academic Press; 2021. p. 103–77. Editor.
- [13] Márquez FPG, Chacón AMP. A review of non-destructive testing on wind turbine blades. *Renew Energy* 2020;161:998–1010.
- [14] Ren Z, et al. Offshore wind turbine operations and maintenance: a state-of-the-art review. *Renewable Sustainable Energy Rev* 2021;144:110886.
- [15] Dalili N, Edrissy A, Cariveau R. A review of surface engineering issues critical to wind turbine performance. *Renewable Sustainable Energy Rev* 2009;13(2):428–38.
- [16] Yang B, Sun D. Testing, inspecting and monitoring technologies for wind turbine blades: a survey. *Renewable Sustainable Energy Rev* 2013;22:515–26.
- [17] Young, A., et al., *Hyperspectral Imaging for Erosion Detection in Wind Turbine Blades*. 2016.
- [18] Rizk P, et al. Wind turbine blade defect detection using hyperspectral imaging. *Remote Sensing Applications: Society and Environment* 2021;22:100522.
- [19] Rizk P, et al. Wind turbine ice detection using hyperspectral imaging. *Remote Sensing Applications: Society and Environment* 2022;26:100711.
- [20] Movsessian A, Cava DG, Tcherniak D. An artificial neural network methodology for damage detection: demonstration on an operating wind turbine blade. *Mech Syst Signal Process* 2021;159:107766.
- [21] Rizk, F., et al., *MAGAN: a Meta-Analysis for Generative Adversarial Networks' Latent Space*. 2023.
- [22] Reddy A, et al. Detection of Cracks and damage in wind turbine blades using artificial intelligence-based image analytics. *Measurement* 2019;147:106823.
- [23] Choung J, et al. Automatic Discontinuity Classification of Wind-turbine Blades Using A-scan-based Convolutional Neural Network. *J. Modern Power Syst. Clean Energy* 2021;9(1):210–8.
- [24] Zhang J, Cosma G, Watkins J. Image Enhanced Mask R-CNN: a Deep Learning Pipeline with New Evaluation Measures for Wind Turbine Blade Defect Detection and Classification. *J. Imaging* 2021;7(3):46.
- [25] Wang M-H, et al. Fault Detection of Wind Turbine Blades Using Multi-Channel CNN. *Sustainability* 2022;14(3):1781.
- [26] Zhu Y, Liu X. A Lightweight CNN for Wind Turbine Blade Defect Detection Based on Spectrograms. *Machines* 2023;11(1):99.
- [27] Guo J, et al. Damage identification of wind turbine blades with deep convolutional neural networks. *Renew Energy* 2021;174:122–33.
- [28] Hacıfendioglu K, et al. Intelligent ice detection on wind turbine blades using semantic segmentation and class activation map approaches based on deep learning method. *Renew Energy* 2022;182:1–16.
- [29] Zare S, Ayati M. Simultaneous fault diagnosis of wind turbine using multichannel convolutional neural networks. *ISA Trans* 2021;108:230–9.
- [30] Ravikanth L, et al. Extraction of Spectral Information from Hyperspectral Data and Application of Hyperspectral Imaging for Food and Agricultural Products. *Food Bioproc Tech* 2017;10(1):1–33.
- [31] Olsen E, Flø A. Spectral and spatially resolved imaging of photoluminescence in multicrystalline silicon wafers. *Appl Phys Lett* 2011;99(1).
- [32] Ma WK, et al. Signal and Image Processing in Hyperspectral Remote Sensing [From the Guest Editors]. *IEEE Signal Process Mag* 2014;31(1):22–3.
- [33] Khan MJ, et al. Modern Trends in Hyperspectral Image Analysis: a Review. *IEEE Access* 2018;6:14118–29.
- [34] Kang Z, et al. Advances in machine learning and hyperspectral imaging in the food supply chain. *Food Eng Rev* 2022;14(4):596–616.
- [35] Chatterjee J, Dethlefs N. Scientometric review of artificial intelligence for operations & maintenance of wind turbines: the past, present and future. *Renewable and Sustainable Energy Reviews* 2021;144:111051.
- [36] Movsessian A, Cava DG, Tcherniak D. An artificial neural network methodology for damage detection: demonstration on an operating wind turbine blade. *Mech Syst Signal Process* 2021;159:107766.

- [37] Calvini R, Ulrici A, Amigo JM, Amigo JM. *Chapter 3.9 - Growing applications of hyperspectral and multispectral imaging, in data handling in science and technology*. Elsevier; 2019. p. 605–29. Editor.
- [38] Yao D, et al. Deep hybrid: multi-graph neural network collaboration for hyperspectral image classification. *Defence Technology* 2023;23:164–76.
- [39] Modarres C, et al. Convolutional neural networks for automated damage recognition and damage type identification. *Structural Control and Health Monitoring* 2018;25(10):e2230.
- [40] Mei S, et al. Learning Sensor-Specific Spatial-Spectral Features of Hyperspectral Images via Convolutional Neural Networks. *IEEE Trans Geosci Remote Sens* 2017; 55(8):4520–33.
- [41] Muniipalle VK, Nelakuditi UR, Nidamanuri RR. Impact of Dimensionality Reduction Techniques on Classification of Hyperspectral Images. In: 2023 3rd International Conference on Intelligent Technologies (CONIT); 2023.
- [42] Chin TJ, Suter D. Incremental Kernel Principal Component Analysis. *IEEE Trans Image Process* 2007;16(6):1662–74.
- [43] Dagher I. Incremental PCA-LDA algorithm. In: 2010 IEEE International Conference on Computational Intelligence for Measurement Systems and Applications; 2010.
- [44] Vecchi DD, Harb M, Dell'Acqua F. A PCA-based hybrid approach for built-up area extraction from Landsat 5, 7 and 8 datasets. In: 2015 IEEE International Geoscience and Remote Sensing Symposium (IGARSS); 2015.
- [45] Mustaqeem M, Saqib M. Principal component based support vector machine (PC-SVM): a hybrid technique for software defect detection. *Cluster Comput* 2021;24 (3):2581–95.
- [46] Li H, et al. A hybrid approach to automatic clustering of white matter fibers. *Neuroimage* 2010;49(2):1249–58.
- [47] Alorfi AA. *Performance evaluation of the PCA versus improved PCA (IPCA) in image compression, and in face detection and recognition*. In: 2016 Future Technologies Conference (FTC); 2016.
- [48] Dou Q, et al. Multilevel Contextual 3-D CNNs for False Positive Reduction in Pulmonary Nodule Detection. *IEEE Trans Biomed Eng* 2017;64(7):1558–67.
- [49] Liu Y, Pu H, Sun D-W. Efficient extraction of deep image features using convolutional neural network (CNN) for applications in detecting and analysing complex food matrices. *Trends Food Sci Technol* 2021;113:193–204.
- [50] Hara K, Kataoka H, Satoh Y. Can spatiotemporal 3d cnns retrace the history of 2d cnns and imagenet?. In: Proceedings of the IEEE conference on Computer Vision and Pattern Recognition; 2018.
- [51] Ning F, et al. Manufacturing cost estimation based on a deep-learning method. *J Manuf Syst* 2020;54:186–95.
- [52] Vapnik VN. An overview of statistical learning theory. *IEEE Trans Neural Networks* 1999;10(5):988–99.
- [53] Bentéjac C, Csörgő A, Martínez-Muñoz G. A comparative analysis of gradient boosting algorithms. *Artif Intell Rev* 2021;54(3):1937–67.
- [54] Carneiro T, et al. Performance Analysis of Google Colaboratory as a Tool for Accelerating Deep Learning Applications. *IEEE Access* 2018;6:61677–85.